

# Germinal centers in human lymph nodes contain reactivated memory B cells

Richard J. Bende, Febe van Maldegem, Martijn Triesscheijn, Thera A.M. Wormhoudt, Richard Guijt, and Carel J.M. van Noesel

Department of Pathology, Academic Medical Center, 1105 AZ Amsterdam, Netherlands

**To reveal migration trails of antigen-responsive B cells in lymphoid tissue, we analyzed immunoglobulin (Ig)M-V<sub>H</sub> and IgG-V<sub>H</sub> transcripts of germinal center (GC) samples microdissected from three reactive human lymph nodes. Single B cell clones were found in multiple GCs, one clone even in as many as 19 GCs. In several GCs, IgM and IgG variants of the same clonal origin were identified. The offspring of individual hypermutated IgG memory clones were traced in multiple GCs, indicating repeated engagement of memory B cells in GC reactions. These findings imply that recurring somatic hypermutation progressively drives the Ig repertoire of memory B cells to higher affinities and infer that transforming genetic hits in non-Ig genes during lymphomagenesis do not have to arise during a single GC passage, but can be collected during successive recall responses.**

## CORRESPONDENCE

C.J.M. van Noesel:  
c.j.vannoessel@amc.uva.nl

Abbreviations used: Ag, antigen(ic); CDR3, complementarity determining region 3; CSR, class-switch recombination; FM, follicular mantle zone; GC, germinal center; IgV, Ig variable region; SHM, somatic hypermutation; TZ, T cell zone.

The humoral immune response relies on mature B cells, each producing a unique Ig. After a primary antigenic (Ag) challenge, triggered naive B cells can differentiate directly into plasma cells producing a first wave of specific, low-affinity IgM antibodies. In parallel, germinal center (GC) reactions are initiated that are critically dependent on T helper cells and are essential to generate B cells with high-affinity antibodies of different classes and to produce memory cells. During the GC reaction, B cells undergo a phase of brisk cell division thereby creating the GC dark zone (1–3). These rapidly dividing cells, centroblasts, accumulate nucleotide substitutions in their Ig variable region (*IgV*) genes, a process designated as somatic hypermutation (SHM) (4–6). Based on competition for survival signals elicited by native Ag presented at the surface of follicular dendritic cells, B cells with Ig variants with the highest affinities obtain growth advantage in the GC light zone (7). In addition, the Ag-selected B cells may switch Ig class due to a genomic recombination process at the *IgH* locus by which the rearranged V<sub>H</sub> region is juxtaposed to one of the downstream C $\gamma$ 3, C $\gamma$ 1, C $\alpha$ 1, C $\gamma$ 2, C $\gamma$ 4, C $\epsilon$ , or C $\alpha$ 2 constant region genes (8). The selected Ig affinity-matured B cells, whether or not class-switched, finally differentiate into antibody-producing plasma cells or memory B cells (2, 3).

The kinetics of the GC reaction have been extensively studied in rodents after immunization with sheep red blood cells or with haptens coupled to carrier proteins. Immunization experiments with T cell-dependent Ags revealed that recognizable GCs are formed within 4–5 d and are maintained for  $\sim$ 21 d (1–3, 9, 10). In spleens from mice immunized with (4-hydroxy-3-nitrophenyl)acetyl coupled to chicken gamma globulin, SHM in the GCs was detectable starting from day 8 to reach approximately three mutations on average per *IgV<sub>H</sub>* gene by day 14. Based on stringent selection, GCs finally become oligoclonal and are reported to contain three to six Ag-specific B cell clones on average (11). In man, in situ analyses on LNs (12, 13) and Peyer's patches (14) showed that the GCs contained 4–13 B cell clones with functional *IgV<sub>H</sub>*. As yet, it is uncertain whether B cells can engage in a GC reaction more than once. In secondary anti-arsenate responses in mice, GC B cells were found to carry higher numbers of somatic mutations in their *IgV<sub>H</sub>* genes as compared with the primary response, whereas affinity-enhancing mutations seemed to appear more rapidly. It remained unclear, however, whether this was due to accelerated SHM rates or recruitment of memory B cells into these responses (15). At least two groups have reported that in man the *IgV<sub>H</sub>* mutation frequencies in both peripheral B cells and intestinal plasma cells increase with age, suggesting repeated rounds of Ag-driven hypermutation (16, 17).

The online version of this article contains supplemental material.

To gain insight in the expansion and dissemination of Ag-responsive B cells in man, we analyzed the clonal B cell composition of 48 GCs of reactive LNs originating from three donors. We observed that single B cell clones seed into multiple GCs, often located at considerable distances, and evidence was obtained for active class-switch recombination (CSR) of B cell clones within individual GCs. Importantly, in the LNs of three donors we encountered the offspring of single, hypermutated IgG clones in multiple GCs, indicative of repeated involvement of Ag-experienced B cells in this unique microenvironment.

## RESULTS

### Laser-aided microdissection and IgV<sub>H</sub> amplification of GC B cells

Small tissue samples of 40–80 cells were isolated out of hematoxylin-stained, frozen sections of three reactive LNs from different donors. To distinguish GCs with cycling B cells, adjacent sections were immunohistochemically stained for the proliferation marker Ki-67. Thus, we microdissected tissue samples of 30, 11, and 16 GCs out of sections of LN1, LN2, and LN3, respectively. As controls, samples from follicular mantle zones (FMs) surrounding the GCs and samples from T cell zones (TZs) were collected. IgV<sub>H</sub> transcripts were amplified by RT-PCR using VH1, VH3, and VH4 family-specific leader primers in combination with a fluorochrome-labeled C<sub>μ</sub> primer, allowing analysis by “genescanning” on automated capillary sequencing equipment (18). Based on length variability of the complementarity determining regions 3 (CDR3s), the samples generally yielded multiple peaks, representing different B cell clones (not depicted). In LN1, we observed in 19 GCs a recurrent 481-bp peak in the VH4-C<sub>μ</sub> PCR (Fig. 1). In LN3, products of the

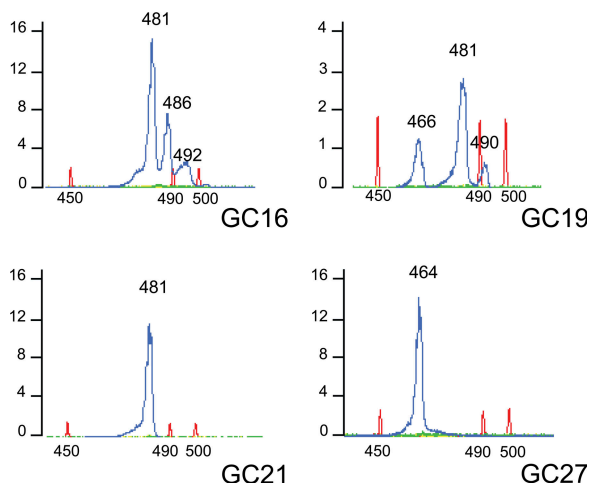


**Figure 1. Genescanning analyses of the IgM-VH4 transcripts amplified out of four individual GC samples of LN1.** Shown are four representative examples of genescanning analyses of IgM-VH4 transcripts present in microdissected tissue samples and amplified by RT-PCR. On the x axis are the lengths in basepairs as determined using internal length markers. The recurrent A- $\mu$  clone with an IgM-VH4 PCR product length of 481 bp is found in GC16, GC19, and in GC21, but not in GC27. These findings correlated well with the cloning experiments separately performed.

same lengths were obtained out of GC1 and GC2 in the VH1-C<sub>μ</sub> PCR (not depicted). We thus decided to extensively clone and sequence VH4-C<sub>μ</sub> PCR products of LN1 and LN2 and VH1-C<sub>μ</sub> PCR products of LN3. RT-PCR products that were used for cloning were generated in parallel using an unlabeled C<sub>μ</sub> primer. Depending on the availability of material, IgG transcripts were also amplified, cloned, and sequenced.

### The offspring of single B cell clones inhabits multiple follicles

Out of most samples, IgV<sub>H</sub> products of different lengths were amplified representing B cell clones with unique IgV<sub>H</sub> compositions. Interestingly, by PCR and cloning we now identified in LN1 and LN3 as many as seven distinct IgM clones of which the offspring was detected in more than one GC. In LN3, four IgM-VH1 clones were identified, termed B- $\mu$ , C- $\mu$ , D- $\mu$ , and G- $\mu$ , which were each present in two GCs (Fig. 2 and Fig. S1, which is available at <http://www.jem.org/cgi/content/full/jem.20071006/DC1>). The B- $\mu$  clone, found in GC1 and GC2 of LN3, comprised 14 subclones (each designated by additive lowercase letters, Ba–Bn), with amino acid sequence differences in their IgV<sub>H</sub>-CDR3. Of this major “B” clone, both IgM- as well as IgG-expressing variants were detected (see below and Figs. S2 and S3). In the two GCs, the Bg- $\mu$  subclone was found.

In the 24 GCs isolated from two separate sections of LN1, three recurrent IgM-VH4 clones were identified, designated

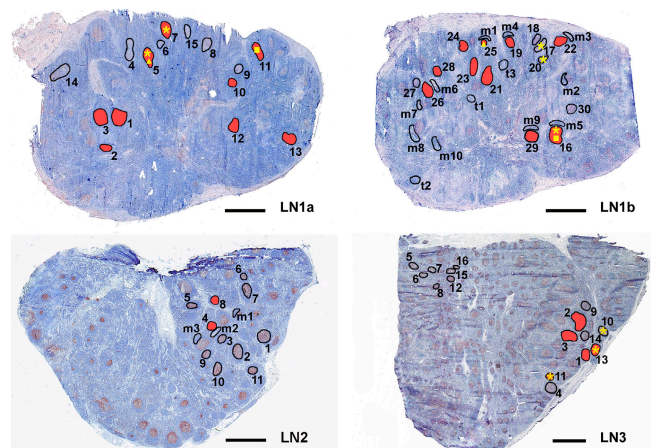


**Figure 2. Localization of recurrent IgM and IgG clones in LNs 1, 2, and 3.** To visualize the proliferating B cells within GCs, the LN sections were immunohistochemically stained for Ki67 (red) and subsequently counterstained with hematoxylin (blue). LN1: The red-filled circles indicate the 19 GCs in which the IgM-VH4 A- $\mu$  clone was found. GCs highlighted by a yellow triangle (GC5 and GC25) and by a yellow box (GC11 and GC16) contained the IgM-VH4 H- $\mu$  and I- $\mu$  clones, respectively. GCs highlighted by a yellow star (GC5, 7, 16, 17, and 20) contained the recurrent IgG-VH4 C- $\gamma$  clone. LN2: The red-filled GC4 and GC8 harbored the IgG-VH4 G- $\gamma$  clone. LN3: The red-filled GCs harbored the four recurrent IgM-VH1 clones, i.e., the B- $\mu$  clone in GC1 and GC2, the C- $\mu$  clone in GC2 and GC3, and the D- $\mu$  and G- $\mu$  clones, both detected in GC11 and GC13. GCs marked by a yellow star (GC10, 11, and 13) contained the recurrent IgG-VH1 J- $\gamma$  clone. Samples from FMs and TZs are indicated by m and t, respectively. Bars, 2 mm.

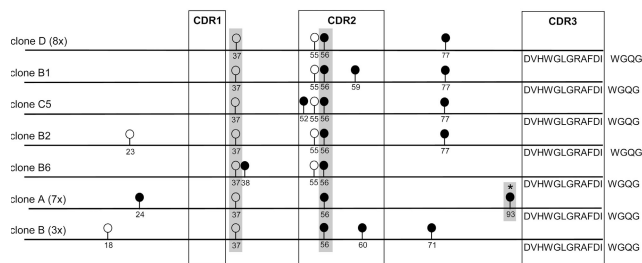
A- $\mu$ , H- $\mu$ , and I- $\mu$ . The H- $\mu$  and I- $\mu$  clones were each present in two GCs. Most striking was the recurrent A- $\mu$  clone, which was traced both by genescanning and sequencing in 19 GCs (Figs. 1 and 2). In all the LN1 samples containing the A- $\mu$  clone, two identical nucleotide substitutions in the rearranged V4-30.4 *IgV<sub>H</sub>* gene were observed, i.e., one silent (S) mutation at codon 37 of FR2 and one replacement (R) mutation at codon 56 of the CDR2. In 5 of the 19 GCs (GC7, 10, 12, 13, and 25), we detected clones containing these two “basic” mutations only, whereas in 14 GCs (GC1, 2, 3, 5, 11, 16, 19, 21, 22, 23, 24, 26, 28, and 29), daughter clones with additional mutations were detected (Fig. 3 and Fig. S4, which is available at <http://www.jem.org/cgi/content/full/jem.20071006/DC1>). All A- $\mu$  clones of GC11 contained an extra R mutation at codon 93. A dissimilar mutation at codon 93 was detected in seven clones derived from GC3 (subclones A) and in one clone from GC5 (subclone 1G1). This may be coincidental or due to selection for binding of an identical Ag epitope. Codon 93 is part of an RGYW motif, the preferential target sequence of the hypermutation machinery (Fig. 3 and Fig. S4; reference 19). Importantly, the A- $\mu$  clone was not detected in the tissue samples from the TZs nor from the FMs, with the exception of the FM7 sample. In the latter, two A- $\mu$  clones were detected out of a total of 26 sequenced IgM-V<sub>H</sub> clones. Overall,

shared mutations between the GC samples were found in four of the seven recurrent clones, i.e., the A- $\mu$  and H- $\mu$  clones of LN1 and the C- $\mu$  and G- $\mu$  clones of LN3 (Figs. S1 and S4).

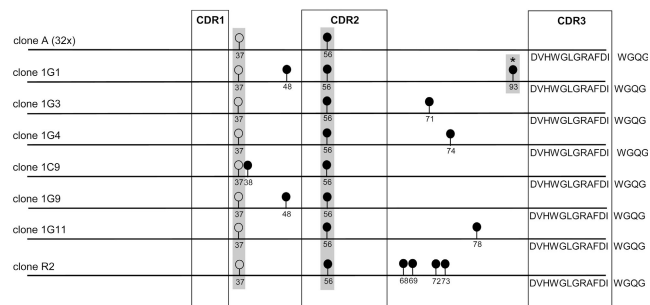
### GCs contain isotype-switch variants of individual B cell clones

Within individual GCs of LN1, LN2, and LN3, a total of 11 IgV<sub>H</sub> clones were identified of which both IgM and IgG variants were present. In 8 of these 11 clonotypic IgM/IgG sets, at least one replacement mutation in the *IgV<sub>H</sub>* gene was shared between the IgM and IgG transcripts (Fig. 4). Interestingly, in GC16 and GC19 of LN1, IgG transcripts of the A- $\mu$  clone were detected. Small amino acid sequence differences in the IgV<sub>H</sub>-CDR3 regions were observed between some of the clonal IgM/IgG sets, i.e., in GC16 (clone A- $\mu$ ), GC19 (clone D), and in GC20 (clone E) of LN1 (Fig. 4 A) and in GC13 (clone F) of LN3 (Fig. 4 C). Of note, the IgM and IgG variants of the Bh subclone in GC1 of LN3 belong to the already mentioned large clone B of which the IgM-expressing Bg- $\mu$  subclone was found in GC1 and GC2. As judged by IgV<sub>H</sub>-CDR3 differences, we identified 11 IgM-, 4 IgG-, and 1 IgM/IgG-expressing variants of this major B clone, which were all found in GC1 and GC2 of LN3 (Fig. 4 C and Figs. S2 and S3).

#### GC3, Clone A- $\mu$

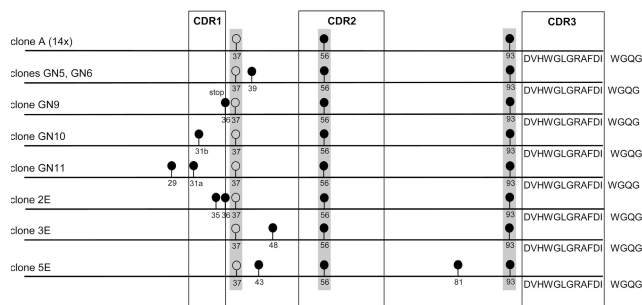


#### GC5, Clone A- $\mu$



Not shown: GC5 contained 5 additional clones with extra mutations

#### GC11, Clone A- $\mu$



#### GC23, Clone A- $\mu$

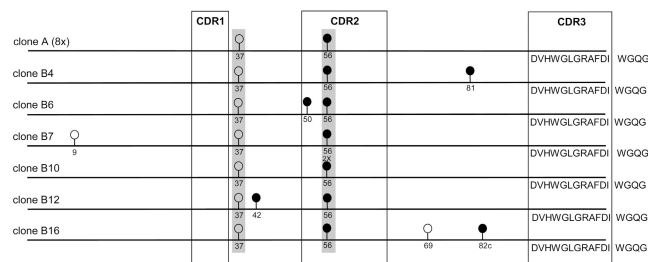


**Figure 3.** Selection of the IgM-V<sub>H</sub>4 sequences and mutations therein of the recurrent A- $\mu$  clone in four GCs of LN1. Lollipop-shaped symbols indicate nucleotide differences as compared with the V4-30.4 germline *IgV<sub>H</sub>* gene. Replacement and silent mutations are indicated by closed and open circles, respectively. Gray shaded bars at codons 37 and 56 indicate identical somatic mutations found in all A- $\mu$  clones. The gray shaded mutation at codon 93 in GC3 and GC5 represents an identical mutation that differed from the codon 93 mutation found in all A- $\mu$  clones of GC11. The total number of clones in which a particular IgV<sub>H</sub> mutation pattern was found is indicated by (Nx).

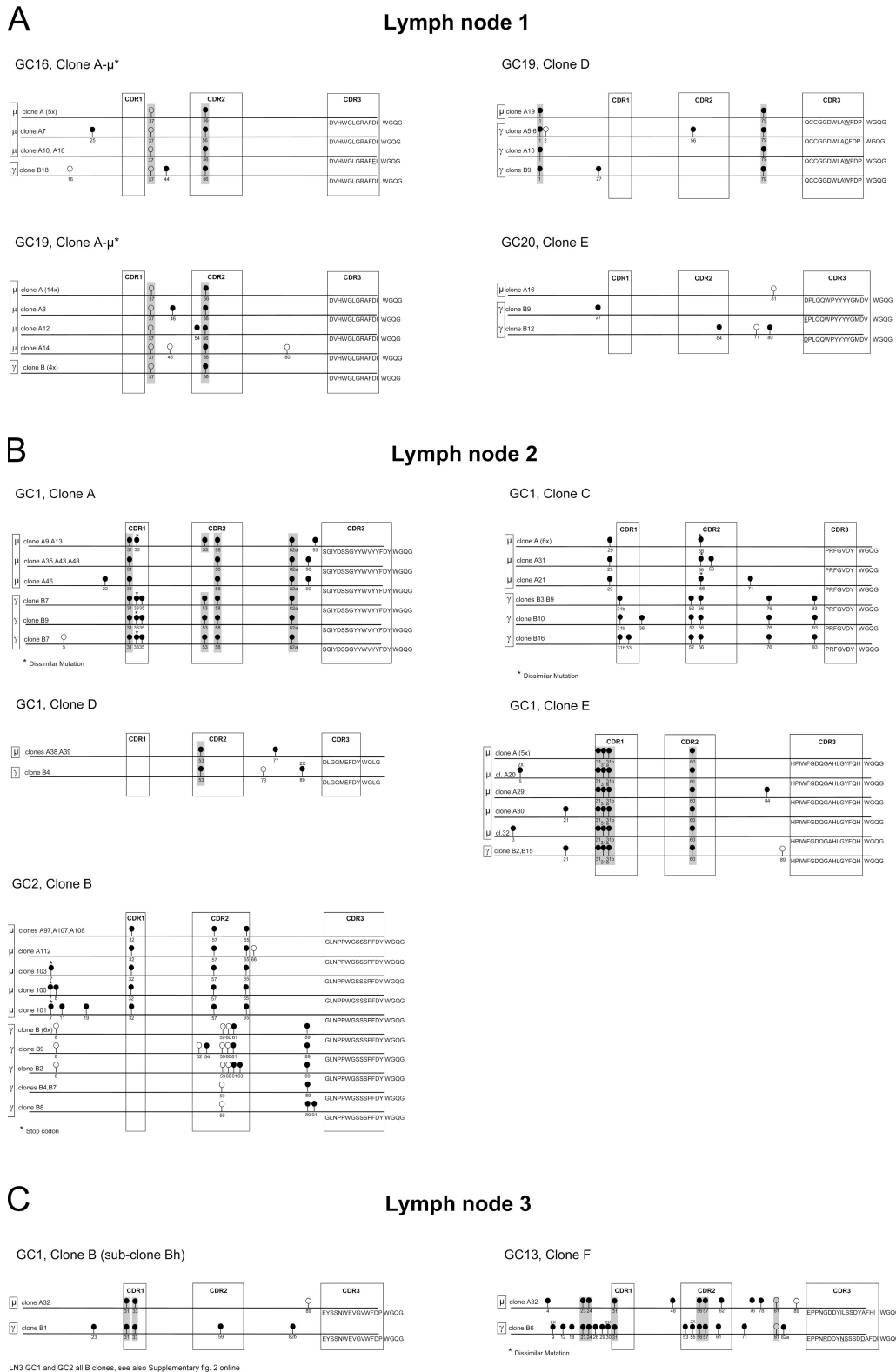


**Figure 4.** IgV<sub>H</sub> sequences and mutations therein of related IgM and IgG clones found within individual GCs of LNs 1, 2, and 3. Lollipop-shaped symbols indicate nucleotide differences as compared with the respective germline IgV<sub>H</sub> genes. Replacement and silent mutations are indicated by closed and open circles, respectively. Gray shaded bars covering mutations of IgM and IgG clones indicate identical mutations. The total number of clones in which a particular IgV<sub>H</sub> mutation pattern was found is indicated by (Nx).

### IgM- and IgG-expressing B cells have different mutation frequencies

Out of LN1, LN2, and LN3, we analyzed 48 different GCs, 18 FMs, and 3 TZs. Thus, a total of 739 IgM-V<sub>H</sub> and 524 IgG-V<sub>H</sub> sequences of the GC samples and 370 and 48 IgM-V<sub>H</sub> sequences of the FM and TZ samples were obtained (Table I). The number of unique IgV<sub>H</sub> clones detected per GC varied from 1 to as many as 14 (GC1 of LN2; Tables S1–S3, available at <http://www.jem.org/cgi/content/full/jem.20071006/DC1>). The average number of mutations of GC IgM clones and of GC IgG clones was 4.1 and 7.4 per IgV<sub>H</sub>, respectively (Fig. 5). Of note, a mutation frequency difference was also found when IgM and IgG sequences, whether or not clonally related, of individual GCs were compared (Fig. 6). In a minority of GCs only, higher mean numbers of IgV<sub>H</sub> mutations were observed in IgM clones as compared with the IgG clones, i.e., in GC1, 24, 25, and 27 of LN1, GC5 of LN2, and in GC10 and 13 of LN3 (Table I). As expected, the IgM-V<sub>H</sub> clones isolated from the FM samples harbored hardly, if any, somatic mutations, i.e., 0.8 mutations per IgV<sub>H</sub> on average. The IgM-V<sub>H</sub> clones of the TZ samples of LN1 harbored on average 3.5 mutations per IgV<sub>H</sub> (Fig. 5). When applying an arbitrary cut off of one or fewer mutations per IgV<sub>H</sub>, unmutated IgM-expressing B cell clones were identified in 24 of the 46 GCs examined (52%). Interestingly, unmutated IgG-expressing B cell clones were identified as well in 8 of the 33 GCs examined (24%). Moreover, applying the same cut off criterion, we found overall 22% unique mutated IgM clones in the FMs, 61% mutated IgM and 90% mutated IgG clones in the GCs, and 56% mutated IgM clones in the TZs, respectively (Tables S1–S6).

### The offspring of single hypermutated IgG B cell clones is present in multiple GCs

In addition to the IgM clones A- $\mu$ , H- $\mu$ , and I- $\mu$  of LN1 and B- $\mu$ , C- $\mu$ , D- $\mu$ , and G- $\mu$  of LN3, we also encountered three IgG-V<sub>H</sub>-expressing clones in multiple GCs of all three LNs.

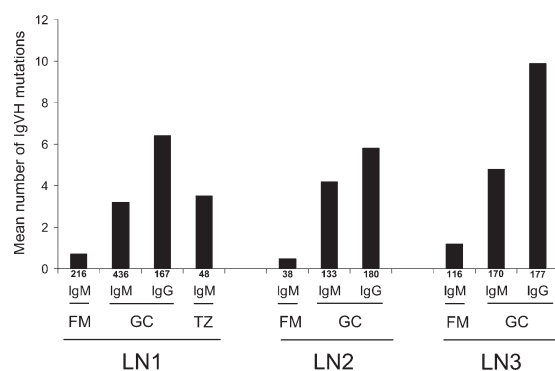


**Figure 5.** Mean IgV<sub>H</sub> mutation numbers of all clones analyzed ordered according to anatomical location in LNs 1, 2, and 3. FM, mantle zones; GC, samples from germinal centers; TZ, samples from T cell areas. Numbers underneath the base of the bars indicate the number of sequenced clones.

In GC5, 7, 16, 17, and 20 of LN1, the offspring of a heavily mutated VH4-IgG-V<sub>H</sub> clone termed C- $\gamma$  was detected. In the five GCs mentioned, the daughter C- $\gamma$  clones contained mean numbers of 29.0, 17.5, 16.6, 16.3, and 25.0 mutations, respectively. As many as nine mutations were shared between all the C- $\gamma$  clones (Figs. 2 and 7). In GC4 and 8 of LN2, a recurrent VH4-IgG-V<sub>H</sub> clone termed G- $\gamma$  was found. All G- $\gamma$  clones harbored one shared mutation. Similarly, in LN3 one recurrent hypermutated VH1-IgG-V<sub>H</sub> clone, J- $\gamma$ , was detected in GC10, 11, and 13. Except for two clones in GC10 (J- $\gamma$  subclones A2 and A5), all the daughter clones of J- $\gamma$  harbored two shared replacement mutations in IgV<sub>H</sub>. In addition, some J- $\gamma$  clones showed differences of their IgV<sub>H</sub>-CDR3s as compared with the consensus CDR3 sequence (J- $\gamma$  subclones A2 and A13 of GC10) (Figs. 2 and 7).

### DISCUSSION

Our *in situ* analyses on the reactive human LNs point out that the B cell response is a highly dynamic process based on entrance and reentrance of single naive and memory B cell clones in multiple GCs. The RT-PCR approach to amplify IgV<sub>H</sub> genes was chosen to be able to discriminate between IgM- and IgG-expressing B cells, information that cannot be obtained by using genomic DNA. We were aware of a potential bias due to intra-GC plasmacytoid cells as they produce disproportionately more Ig per cell. Immunohistochemical stainings indicated that in the GCs of LN1 and LN2, CD138 (syndecan-1)-expressing plasma cells were virtually absent, whereas they were abundantly present in the extrafollicular areas. In LN3, ~50% of the GCs did contain scattered plasmacytoid cells, weakly expressing CD138 (Fig. S6, available at <http://www.jem.org/cgi/content/full/jem.20071006/DC1>). Intra-GC plasmacytoid cells are, for several reasons, unlikely to be just random follicular immigrants but are rather maturing locally and thus are a direct reflection of the Ag-stimulated GC B cell population. Extrafollicular differentiating plasma cells up-regulate CD138 and down-regulate receptors that

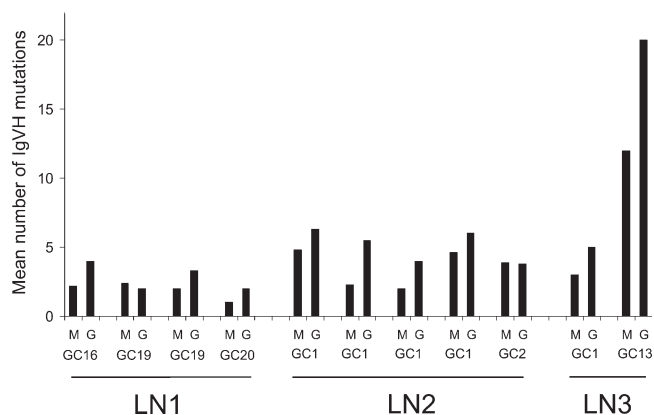


**Figure 6.** Mean IgV<sub>H</sub> mutation numbers of related IgM and IgG clones found within individual GCs. The mean IgV<sub>H</sub> mutation numbers of the 11 clonal IgM/IgG sets of Fig. 4 are shown. M and G indicate related IgM and IgG clones, respectively.

**Table I.** IgV<sub>H</sub> clones found in samples microdissected out of three reactive human LNs

	GC samples	Amplified Ig transcripts	No. of RT-PCR	Clones sequenced	Mean no. of IgVH mutations of all clones
LN 1	GC1 <sup>a</sup>	VH4-IgM	5	47	2.3
	GC1 <sup>a</sup>	VH4-IgG	1	15	0.5
	GC2 <sup>a</sup>	VH4-IgM	7	74	1.9
	GC3 <sup>a</sup>	VH4-IgM	3	22	4.3
	GC5 <sup>a</sup>	VH4-IgM	9	53	2.6
	GC5 <sup>a</sup>	VH4-IgG	2	5	29.0
	GC7	VH4-IgM	1	6	2.0
	GC7	VH4-IgG	1	6	5.8
	GC10	VH4-IgM	1	7	2.0
	GC10	VH4-IgG	1	7	3.4
	GC11	VH4-IgM	3	22	3.5
	GC11	VH4-IgG	2	18	6.8
	GC12	VH4-IgM	1	2	2.0
	GC13 <sup>a</sup>	VH4-IgM	2	13	2.0
	GC16	VH4-IgM	1	15	2.4
	GC16	VH4-IgG	1	25	10.3
	GC17	VH4-IgM	1	13	0.3
	GC17	VH4-IgG	1	18	6.3
	GC18	VH4-IgM	1	14	4.9
	GC18	VH4-IgG	1	6	8.0
	GC19	VH4-IgM	1	17	2.1
	GC19	VH4-IgG	1	16	4.7
	GC20	VH4-IgM	1	5	1.8
	GC20	VH4-IgG	1	14	4.3
	GC21	VH4-IgM	1	15	2.3
	GC22	VH4-IgM	1	15	1.7
	GC23	VH4-IgM	1	14	2.3
	GC24	VH4-IgM	1	14	1.9
	GC24	VH4-IgG	1	8	1.5
	GC25	VH4-IgM	1	11	3.1
	GC25	VH4-IgG	1	16	1.6
	GC26	VH4-IgM	1	14	2.6
	GC27	VH4-IgM	1	14	21.1
	GC27	VH4-IgG	1	12	1.3
	GC28	VH4-IgM	1	12	2.3
	GC29	VH4-IgM	1	9	2.7
	GC30	VH4-IgM	1	8	1.3
	FM1	VH4-IgM	1	23	0.2
	FM2	VH4-IgM	1	8	0.1
	FM3	VH4-IgM	1	27	0.0
FM4	VH4-IgM	1	26	0.2	
FM5	VH4-IgM	1	26	1.6	
FM6	VH4-IgM	1	23	0.5	
FM7 <sup>a</sup>	VH4-IgM	2	26	1.5	
FM8 <sup>a</sup>	VH4-IgM	2	28	1.8	
FM9	VH4-IgM	1	6	0.8	
FM10	VH4-IgM	1	23	0.3	
TZ1	VH4-IgM	1	12	4.7	
TZ2	VH4-IgM	1	16	3.1	
TZ3	VH4-IgM	1	20	2.8	
LN 2	GC1 <sup>b</sup>	VH4-IgM	4	51	2.8
	GC1 <sup>b</sup>	VH4-IgG	6	66	6.0

**Table I.** IgV<sub>H</sub> clones found in samples microdissected out of three reactive human LNs (*Continued*)

	GC samples	Amplified Ig transcripts	No. of RT-PCR	Clones sequenced	Mean no. of IgVH mutations of all clones
	GC2 <sup>b</sup>	VH4-IgM	2	15	2.1
	GC2 <sup>b</sup>	VH4-IgG	6	44	5.2
	GC3	VH4-IgM	1	9	1.6
	GC4	VH4-IgM	1	16	4.4
	GC4	VH4-IgG	1	7	6.9
	GC5	VH4-IgM	1	14	4.7
	GC5	VH4-IgG	2	21	2.9
	GC6	VH4-IgM	1	13	5.2
	GC6	VH4-IgG	2	17	6.1
	GC8	VH4-IgM	1	4	7.8
	GC8	VH4-IgG	1	25	7.9
	GC10	VH4-IgM	1	11	4.9
	FM1	VH4-IgM	1	16	1.1
	FM2	VH4-IgM	1	14	0.1
	FM3	VH4-IgM	1	8	0.3
LN 3	GC1 <sup>c</sup>	VH1-IgM	2	24	7.2
	GC1 <sup>c</sup>	VH1-IgG	2	26	12.7
	GC2	VH1-IgM	1	9	3.6
	GC2	VH1-IgG	1	10	5.1
	GC3	VH1-IgM	1	4	1.3
	GC3	VH1-IgG	1	14	7.0
	GC4	VH1-IgM	1	12	3.6
	GC4	VH1-IgG	1	15	3.6
	GC5	VH1-IgM	1	14	13.0
	GC7	VH1-IgM	1	12	2.8
	GC8	VH1-IgM	1	11	8.2
	GC8	VH1-IgG	1	10	21.3
	GC9	VH1-IgM	1	14	6.4
	GC9	VH1-IgG	1	14	8.0
	GC10	VH1-IgM	1	8	10.5
	GC10	VH1-IgG	1	13	9.2
	GC11	VH1-IgM	1	14	5.2
	GC11	VH1-IgG	1	13	8.1
	GC12	VH1-IgM	1	8	1.6
	GC12	VH1-IgG	1	12	16.3
	GC13	VH1-IgM	1	25	10.5
	GC13	VH1-IgG	1	8	5.4
	GC14	VH1-IgM	1	15	1.7
	GC14	VH1-IgG	1	8	9.4
	GC15	VH1-IgM	1	9	1.3
	GC16	VH1-IgM	1	5	2.4
	GC16	VH1-IgG	1	8	16.3
	GC17 <sup>d</sup>	VH1-IgM	1	12	1.3
	FM1 <sup>d</sup>	VH1-IgM	1	15	2.0
	FM2 <sup>d</sup>	VH1-IgM	1	15	0.2
	FM3 <sup>d</sup>	VH1-IgM	1	14	2.8
	FM4 <sup>d</sup>	VH1-IgM	1	15	0.6
	FM5 <sup>d</sup>	VH1-IgM	1	57	0.3

<sup>a</sup>Of GC2, GC3, GC5, GC13, MZ7, and MZ8, two microdissected samples were analyzed.

<sup>b</sup>Of GC1 and GC2, four and two microdissected samples were analyzed, respectively.

<sup>c</sup>Of GC1, two microdissected samples were analyzed.

<sup>d</sup>The microdissected samples of GC17 and FM1–FM5 are indicated in Fig. S5.

are essential to enter GCs, i.e., membrane-bound Ig to interact with Ag and the follicle-attracting chemokine receptor CXCR5 (20). Moreover, they up-regulate CXCR4 whose ligand (CXCL12/SDF) is highly expressed in the medullary cords (20). Finally, the fact that in several GCs isotype-switch variants of individual B cell clones were detected underscores the solidity of the experimental strategy.

The number of unique VH4- or VH1-expressing clones identified per GC varied between 1 and 14 (GC1 of LN2; Tables S1–S3). Others have reported numbers of unique clones in human GCs, ranging between 4 and 13 and 1 and 16 (12–14), whereas in immunization studies with T cell-dependent Ags in the mouse, averages of 3–6 clones per GC have been documented (11). These combined results are suggestive for a more diverse B cell repertoire in GCs in man, which still is an underestimation because only one *IgV<sub>H</sub>* gene family was analyzed in detail per LN. Furthermore, these findings must be interpreted with caution because in the human system, no information on the kinetics and the stage of the GC reaction studied is available.

In LN1 and LN3, we detected seven distinct IgM-expressing clones that were each present in at least two separate GCs (Figs. 1–3 and Figs. S1 and S2). Most remarkable was the IgM-VH4 A- $\mu$  clone that was traced in 19 of 24 GCs in two consecutive sections of LN1 (Fig. 2). It is emphasized that although the A- $\mu$  clone was detected in the majority of the GC samples, it was found only in 1 of the 10 analyzed samples from adjacent mantle zones and not at all in randomly collected samples from the TZs of LN1. All the A- $\mu$  clones contained two identical mutations, and in 14 GCs daughter clones with unique additional mutations were detected (Fig. 3 and Fig. S4). The finding of the widely disseminated A- $\mu$  clone in LN1 is in accordance with studies in mice showing that after a primary immunization with the hapten arsonate, some clonotypic B cells expanded and subsequently populated different follicles in which the daughter cells underwent their own clonal evolution (15). Extrafollicular proliferation has also been demonstrated in mice immunized with (4-hydroxy-3-nitrophenyl)acetyl coupled to chicken gamma globulin. In this system, unmutated and mutated daughter cells of a B cell clone were found in an extrafollicular plasma cell focus and in a neighboring GC, respectively (21). Thus, two scenarios may explain the presence of IgM clones with shared mutations in multiple GCs, such as the A- $\mu$  clone: (a) Ag activation of a naive IgM precursor B cell, induction of SHM, and, after limited proliferation, migration into multiple primary follicles; and (b) extrafollicular reactivation and proliferation of one or more members of a mutated memory IgM B cell and subsequent seeding into various follicles.

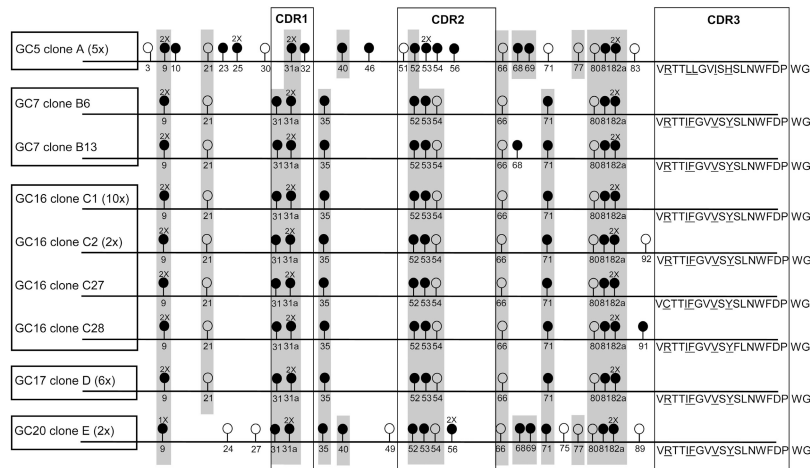
As expected, hypermutated IgV<sub>H</sub> clones were found mainly in the GC samples. In contrast, the mean number of mutations of the IgM clones from FMs did not exceed 0.7

per IgV<sub>H</sub>. Still, the FM samples contained 22% of mutated IgM clones, and, conversely, in the GCs as many as 39% of the IgM clones and 10% of the IgG clones were unmutated. These findings are compatible with previous microdissection studies on human LNs (12, 13) and are explained by recent intravital two-photon microscopy studies. In the latter studies, it was demonstrated that trafficking of naive B cells is not completely restricted to the mantle zones as they frequently surpass the GC borders (22, 23). We found means of 3.2, 4.2, and 4.8 mutations for IgM clones and 6.4, 5.8, and 9.9 mutations for IgG clones in LNs 1, 2, and 3, respectively (Fig. 5). For tonsillar IgM and IgG B cells, average mutation loads of 5.7 and 9.5 have been reported (24). Interestingly, we identified 11 clones of which IgM and IgG isotype variants were present within individual GCs, providing formal proof for active CSR in this environment in man. Shared replacement mutations were identified in 8 out of the 11 paired IgM/IgG clones (Fig. 4). Again, the IgG clones generally contained more mutations as compared with the corresponding IgM clones (Fig. 6). This finding is a priori not expected noticing that the 11 isotype-switch variants each originate from single Ag-responsive precursor cells that had resided for equal times in their particular GCs. Isotype-related mutation differences within GCs can, hypothetically, be explained by a nonrandom process of CSR that is more due at higher IgV affinities and thus stronger BCR signals. However, the finding of unmutated IgG clones in 8 of the 33 GCs examined indicates that such an affinity threshold is not absolute.

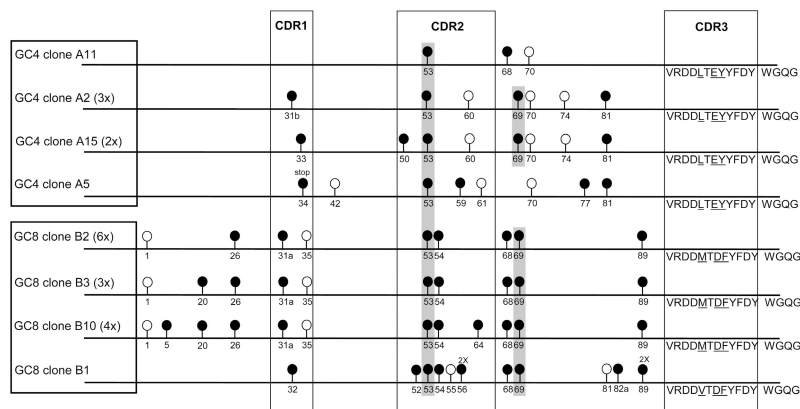
In three LNs, recurrent hypermutated IgG clones were identified, i.e., in LN1 the IgG-VH4 C- $\gamma$  clone in five GCs, in LN2 the IgG-VH4 G- $\gamma$  clone in two GCs, and in LN3 the IgG-VH1 J- $\gamma$  clone in three GCs. Importantly, as many as nine mutations were shared among the C- $\gamma$  clones found in the five GCs, whereas in the J- $\gamma$  clones retrieved from the three GCs, two replacement mutations were common (Fig. 7). This, together with the fact that no corresponding IgM variants were traced, indicates earlier GC passage(s) of precursor clones of C- $\gamma$ , G- $\gamma$ , and J- $\gamma$ . These recurrent IgG-expressing clones are thus to be considered as reactivated memory B cell clones. Repeated GC engagement has been proposed to occur in mice as well. Secondary response to phosphorylcholine-KLH yielded B cells that were more heavily mutated as compared with primary response B cells, whereas most of the mutations appeared to be shared among the clones. This latter observation suggested mere expansion of memory B cells within GCs with minimal additional SHM (25). Recent intravital two-photon microscopic experiments in mice also indicated that memory B cells are able to join an existing GC, provided they have a competitive advantage in Ag binding affinity (23). Repetitive passing of memory B cells through

**Figure 7.** IgV<sub>H</sub> sequences and mutations therein of the recurrent IgG clones found in LNs 1, 2, and 3. The C- $\gamma$  clone found in five GCs of LN1 is shown in the top, the G- $\gamma$  clone found in two GCs of LN2 is shown in the middle, and the J- $\gamma$  clone found in three GCs of LN3 is shown in the bottom. Lollipop-shaped symbols indicate nucleotide differences as compared with the V4-4, V4-30.4, and the V1-69 germline *IgV<sub>H</sub>* genes, respectively. Replacement and silent mutations are indicated by closed and open circles. Gray shaded bars indicate the identical somatic mutations in the different GCs. 2X, two mutations in the indicated codon. The total number of clones in which a particular IgV<sub>H</sub> mutation pattern was found is indicated by Nx.

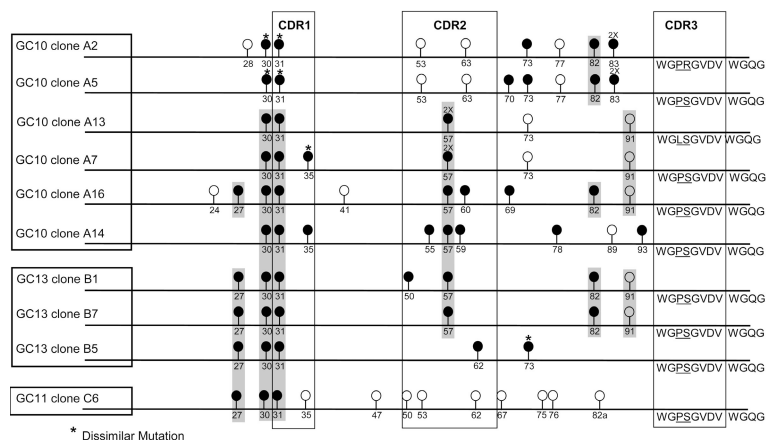
LN1: GC5, GC7, GC16, GC17 and GC20, clone C- $\gamma$



LN2: GC4 and GC8, clone G- $\gamma$



LN3: GC10, GC11 and GC13, clone J- $\gamma$



GCs is compatible with (a) the fact that peripheral blood memory B cells on average harbor higher mutation loads as compared with GC B cells in LN and tonsil (24, 26); (b) the positive correlation between mean  $IgV_H$  mutation frequencies of memory B cells and age (in young and aged humans, respective mean mutation numbers of 9.7 and 11.5 for IgM and 17.3 and 22.5 for IgG memory B cells have been reported [17]); and (c) the reported difference in replication history of memory B cells in children and adults, having undergone  $\sim 8$  and 11 cell divisions, respectively (27). In this respect, it can be envisaged that the relative contribution of memory B cells to GC responses increases with age.

It is generally believed that B cells expanding in GCs are at increased risk of genetic derailment. The facts that lymphomas are in majority of B cell origin, of GC or post-GC phenotype, and carry hypermutated  $IgV_H$  genes support the notion that most lymphomas arise during this turbulent differentiation phase. The processes of SHM and CSR, both accompanied by single- and double-stranded DNA breaks, imply genetic instability and are potentially dangerous because they may act also beyond the Ig locus (28–30). Indeed, ample evidence is now available that many of the chromosomal translocations specific for the various B cell lymphoma entities are byproducts of these two processes (31, 32). So far, the implicit presumption has been that the genetic hits necessary for cellular transformation have to occur during the relatively brief proliferation phase of a single GC reaction. Knowing now that memory B cells reenter secondary follicles, most likely upon renewed Ag challenge, an alternative scenario of B cell lymphomagenesis can be envisaged. Hence, the transforming genetic hits do not have to occur during the first and only GC passage but can, in parallel to the gain of IgV mutations, gradually accumulate in memory B cells during successive recall responses throughout life. This scenario would explain why the peak incidence of B cell non-Hodgkin's lymphoma is not early in life, when most primary responses occur, but at late adulthood long after establishing the memory B cell repertoire. This pathogenetic course is also in accordance with the high  $IgV_H$  mutation frequencies found in all (post) GC B cell lymphomas, i.e., being in the range of those found in peripheral blood memory B cells rather than those of primary GC B cells (17, 24, 26, 33–36). Finally, if true one would expect that B cells belonging to expanded memory clones specific for common pathogens would be most at risk and therefore overrepresented among the various B cell lymphomas. This antigenetic bias should be reflected in the Ig repertoire of (post) GC B cell lymphomas.

## MATERIALS AND METHODS

**Patient material.** All LNs were fresh-frozen in liquid nitrogen shortly after surgical resection. LN1 was a cervical LN removed from a 4-yr-old male suffering from sustained lymphadenopathy, and LN2 originated from the arteria hepatica communis region and had been removed from a 75-yr-old male suffering from pancreatic carcinoma. LN3 was a cervical LN resected out of a 46-yr-old woman suffering from chronic sialadenitis. All LNs contained reactive lymph follicles. Of note, LN2 was purely reactive and did not contain carcinoma cells.

The study was performed in accordance with the ethical standards and approved by the research code committee on human experimentation of our institute.

**Immunohistochemistry.** The immunohistochemical stainings were performed on acetone-fixed cryostat sections using the PowerVision detection system (ImmunoVision Technologies). Endogenous peroxidase activity was blocked with 0.1%  $NaN_3$ , 0.3%  $H_2O_2$  in PBS. Visualization of antibody binding was performed with 3-amino-9-ethylcarbazole (Sigma-Aldrich), 0.03%  $H_2O_2$  in sodium acetate, pH 4.9. A monoclonal antibody specific for Ki-67 (MIB-1; DakoCytomation) was used.

**Laser-aided microdissection and cDNA synthesis.** 10- $\mu m$  frozen tissue sections were mounted on polyethylene membranes (PALM) and briefly stained with hematoxylin for 1 min, followed by gentle rinsing with tap water and finally with distilled water. After air drying, microdissection was performed using the PALM system. Using the 20 $\times$  objective, tissue pieces with a diameter of  $\sim 50 \mu m$  were cut out and catapulted in the cap of a microfuge tube containing 20  $\mu l$  of RT reaction mix. Next, the tubes were incubated, upside down, in direct contact with a heating block at 42°C for 1 h, followed by an inactivation at 95°C for 10 min. The RT mix contained the following: 0.1 mmol/l  $Pd(N)_6$  random primers, 8 U/ $\mu l$  molony murine leukemia virus RT (Invitrogen), 1 mmol/l of each dNTP, and 1.2 U/ $\mu l$  RNase inhibitor (Roche) in 1 $\times$  first strand buffer (Invitrogen).

**$IgV_H$  amplification by RT-PCR, cloning, and sequencing.**  $IgM-V_H$  and  $IgG-V_H$  transcripts were amplified using  $V_H$  family-specific leader primers for the  $VH1$ ,  $VH3$ , and  $VH4$  families of the  $IgV_H$  genes in combination with  $C\mu$  and  $C\gamma$  primers, respectively (37). In some experiments, a fluorochrome-labeled  $C\mu$  primer was used to enable automated detection of PCR products by genescanning with capillary sequencing equipment (18). The PCR was performed with 1  $\mu l$  cDNA in a 25- $\mu l$  volume and started with 4 min at 95°C, followed by 10 cycles of 1 min at 95°C, 30 s at 57°C, and 1 min at 72°C, followed by 40 cycles of 30 s at 95°C, 30 s at 55°C, and 1 min at 72°C. The reaction was terminated for 6 min at 72°C. The PCR was performed in 1.5 mmol/l  $MgCl_2$  using Platinum Taq polymerase and PCR buffers (Invitrogen) according to the manufacturer's description. In each RT-PCR run, water controls were included, which were in all cases negative. Moreover, three control samples of the polyethylene membrane were also tested and turned out to be negative.  $VH1/VH4-IgV_H$  RT-PCR products were cloned into pTOPO-TA vectors and transformed into TOP10 bacteria (Invitrogen) to generate molecular  $IgV_H$  clones. Sequencing on both strands was performed using the big dye terminator cycle sequencing kit (Applied Biosystems). To identify the  $IgV_H$  germline gene used and the somatic mutations therein, the sequences were compared with published germline  $IgV_H$  genes using the Vbase database (38) and DNAPlot online (<http://www.mrc-cpe.cam.ac.uk>).

The Taq error rate in our 50-cycle RT-PCR was experimentally determined in an RT-PCR specific for CD20 using two FM samples of LN1. By sequencing 29 clones, the Taq error rate was found to be  $\sim 0.3$  bp per 300 bp.

**Online supplemental material.** Fig. S1 shows  $IgV_H$  sequences and mutations therein of recurrent IgM clones found in the GCs of LN1 (H- $\mu$  and I- $\mu$ ) and LN3 (B- $\mu$ , C- $\mu$ , D $\mu$ , and G- $\mu$ ). In Fig. S2,  $IgV_H$  sequences of all B- $\mu$  subclones found in GC1 and GC2 of LN 3 are shown. Fig. S3 shows  $IgV_H$ -CDR3 amino acid sequences of all B subclones found in GC1 and GC2 of LN3. Fig. S4 shows  $IgV_H$  sequences of the recurrent A- $\mu$  clone found in 19 GCs of LN1, and Fig. S5 shows microdissected samples of GC17 and FM1-FM5 in an additional section of LN3. In Fig. S6, immunohistochemical detection of CD138 in LNs 1–3 is shown. In Tables S1–S3,  $IgV_H$  rearrangements of all IgM and IgG clones found in the GCs of LNs 1–3 are listed. Tables S4–S6 show  $IgV_H$  rearrangements of all IgM clones found in the FMs and TZs of LNs 1–3.

We thank W.P. Meun for photography, M. Kleijer for technical assistance, and Dr. R.A.W. van Lier and R. Hoogeboom for critical reading of the manuscript.

The authors have no conflicting financial interests.

Submitted: 21 May 2007

Accepted: 17 September 2007

## REFERENCES

- Kroese, F.G., W. Timens, and P. Nieuwenhuis. 1990. Germinal center reaction and B lymphocytes: morphology and function. *Curr. Top. Pathol.* 84:103–148.
- MacLennan, I.C.M. 1994. Germinal centers. *Annu. Rev. Immunol.* 12:117–139.
- Liu, Y.-J., G. Grouard, O. de Bouteiller, and J. Banchereau. 1996. Follicular dendritic cells and germinal centers. *Int. Rev. Cytol.* 166:139–179.
- Berek, C., and C. Milstein. 1988. The dynamic nature of the antibody repertoire. *Immunol. Rev.* 105:5–26.
- Berek, C., A. Berger, and M. Apel. 1991. Maturation of the immune response in germinal centers. *Cell.* 67:1121–1129.
- Jacob, J., G. Kelsoe, K. Rajewsky, and U. Weiss. 1991. Intracлонаl generation of antibody mutants in germinal centres. *Nature.* 354:389–392.
- Lindhout, E., G. Koopman, S.T. Pals, and C. de Groot. 1997. Triple check for antigen specificity of B cells during germinal centre reactions. *Immunol. Today.* 18:573–577.
- Liu, Y.J., F. Malisan, O. de Bouteiller, C. Guret, S. Lebecque, J. Banchereau, F.C. Mills, E.E. Max, and H. Martinez-Valdez. 1996. Within germinal centers, isotype switching of immunoglobulin genes occurs after the onset of somatic mutation. *Immunity.* 4:241–250.
- Liu, Y.-J., J. Zhang, P.J.L. Lane, E.Y.T. Chan, and I.C.M. MacLennan. 1991. Sites of specific B cell activation in primary and secondary responses to T cell-dependent and T cell-independent antigens. *Eur. J. Immunol.* 21:2951–2962.
- Jacob, J., R. Kassir, and G. Kelsoe. 1991. In situ studies of the primary immune response to (4-hydroxy-3-nitrophenyl)acetyl. I. The architecture and dynamics of responding cell populations. *J. Exp. Med.* 173:1165–1175.
- Jacob, J., J. Przylepa, C. Miller, and G. Kelsoe. 1993. In situ studies of the primary immune response to (4-hydroxy-3-nitrophenyl)acetyl. III. The kinetics of V region mutation and selection in germinal center B cells. *J. Exp. Med.* 178:1293–1307.
- Küppers, R., M. Zhao, M.-L. Hansmann, and K. Rajewsky. 1993. Tracing B cell development in human germinal centres by molecular analysis of single cells picked from histological sections. *EMBO J.* 12:4955–4967.
- Roers, A., M.L. Hansmann, K. Rajewsky, and R. Küppers. 2000. Single-cell PCR analysis of T helper cells in human lymph node germinal centers. *Am. J. Pathol.* 156:1067–1071.
- Banerjee, M., R. Mehr, A. Belevovsky, J. Spencer, and D.K. Dunn-Walters. 2002. Age- and tissue-specific differences in human germinal center B cell selection revealed by analysis of IgVH gene hypermutation and lineage trees. *Eur. J. Immunol.* 32:1947–1957.
- Vora, K.A., K. Tumas-Brundage, and T. Manser. 1999. Contrasting the in situ behavior of a memory B cell clone during primary and secondary immune responses. *J. Immunol.* 163:4315–4327.
- Dunn-Walters, D.K., L. Boursier, and J. Spencer. 1997. Hypermutation, diversity and dissemination of human intestinal lamina propria plasma cells. *Eur. J. Immunol.* 27:2959–2964.
- Chong, Y., H. Ikematsu, K. Yamaji, M. Nishimura, S. Kashiwagi, and J. Hayashi. 2003. Age-related accumulation of Ig V(H) gene somatic mutations in peripheral B cells from aged humans. *Clin. Exp. Immunol.* 133:59–66.
- van Dongen, J.J., A.W. Langerak, M. Brüggemann, P.A. Evans, M. Hummel, F.L. Lavender, E. Delabesse, F. Davi, E. Schuurink, R. Garcia-Sanz, et al. 2003. Design and standardization of PCR primers and protocols for detection of clonal immunoglobulin and T-cell receptor gene recombinations in suspect lymphoproliferations: report of the BIOMED-2 Concerted Action BMH4-CT98-3936. *Leukemia.* 17:2257–2317.
- Rogozin, I.B., and N.A. Kolchanov. 1992. Somatic hypermutagenesis in immunoglobulin genes. II. Influence of neighbouring base sequences on mutagenesis. *Biochim. Biophys. Acta.* 1171:11–18.
- Hargreaves, D.C., P.L. Hyman, T.T. Lu, V.N. Ngo, A. Bidgol, G. Suzuki, Y.R. Zou, D.R. Littman, and J.G. Cyster. 2001. A coordinated change in chemokine responsiveness guides plasma cell movements. *J. Exp. Med.* 194:45–56.
- Jacob, J., and G. Kelsoe. 1992. In situ studies of the primary immune response to (4-hydroxy-3-nitrophenyl)acetyl. II. A common clonal origin for periarteriolar lymphoid sheath-associated foci and germinal centers. *J. Exp. Med.* 176:679–687.
- Allen, C.D., T. Okada, H.L. Tang, and J.G. Cyster. 2007. Imaging of germinal center selection events during affinity maturation. *Science.* 315:528–531.
- Schwickert, T.A., R.L. Lindquist, G. Shakhar, G. Livshits, D. Skokos, M.H. Kosco-Vilbois, M.L. Dustin, and M.C. Nussenzweig. 2007. In vivo imaging of germinal centres reveals a dynamic open structure. *Nature.* 446:83–87.
- Pascual, V., Y.-J. Liu, A. Magalski, O. de Bouteiller, J. Banchereau, and J.D. Capra. 1994. Analysis of somatic mutation in five B cell subsets of human tonsil. *J. Exp. Med.* 180:329–339.
- Miller, C., J. Stedra, G. Kelsoe, and J. Cerny. 1995. Facultative role of germinal centers and T cells in the somatic diversification of IgVh genes. *J. Exp. Med.* 181:1319–1331.
- Klein, U., K. Rajewsky, and R. Küppers. 1998. Human immunoglobulin (IgM<sup>+</sup>IgD<sup>+</sup>) peripheral blood B cells expressing the CD27 cell surface antigen carry somatically mutated variable region genes: CD27 as a general marker for somatically mutated (memory) B cells. *J. Exp. Med.* 188:1679–1689.
- van Zelm, M.C., T. Szczepanski, M. van der Burg, and J.J. van Dongen. 2007. Replication history of B lymphocytes reveals homeostatic proliferation and extensive antigen-induced B cell expansion. *J. Exp. Med.* 204:645–655.
- Shen, H.M., A. Peters, B. Baron, X. Zhu, and U. Storb. 1998. Mutation of BCL-6 gene in normal B cells by the process of somatic hypermutation of Ig genes. *Science.* 280:1750–1752.
- Pasqualucci, L., A. Migliozza, N. Fracchiolla, C. William, A. Neri, L. Baldini, R.S. Chaganti, U. Klein, R. Küppers, K. Rajewsky, and R. Dalla-Favera. 1998. BCL-6 mutations in normal germinal center B cells: evidence of somatic hypermutation acting outside Ig loci. *Proc. Natl. Acad. Sci. USA.* 95:11816–11821.
- Pasqualucci, L., P. Neumeister, T. Goossens, G. Nanjangud, R.S. Chaganti, R. Küppers, and R. Dalla-Favera. 2001. Hypermutation of multiple proto-oncogenes in B-cell diffuse large-cell lymphomas. *Nature.* 412:341–346.
- Bende, R.J., L.A. Smit, and C.J. van Noesel. 2007. Molecular pathways in follicular lymphoma. *Leukemia.* 21:18–29.
- Küppers, R. 2005. Mechanisms of B-cell lymphoma pathogenesis. *Nat. Rev. Cancer.* 5:251–262.
- Aarts, W.M., R.J. Bende, E.J. Steenbergen, P.M. Kluin, E.C.M. Ooms, S.T. Pals, and C.J.M. van Noesel. 2000. Variable heavy chain gene analysis of follicular lymphomas: correlation between heavy chain isotype expression and somatic mutation load. *Blood.* 95:2922–2929.
- Bende, R.J., W.M. Aarts, D. de Jong, S.T. Pals, and C.J. van Noesel. 2005. Among B cell non-Hodgkin's lymphomas, MALT lymphomas express a unique antibody repertoire with frequent rheumatoid factor reactivity. *J. Exp. Med.* 201:1229–1241.
- Klein, U., T. Goossens, M. Fischer, H. Kanzler, A. Braeuninger, K. Rajewsky, and R. Küppers. 1998. Somatic hypermutation in normal and transformed human B cells. *Immunol. Rev.* 162:261–280.
- Tsuiji, M., S. Yurasov, K. Velinzon, S. Thomas, M.C. Nussenzweig, and H. Wardemann. 2006. A checkpoint for autoreactivity in human IgM<sup>+</sup> memory B cell development. *J. Exp. Med.* 203:393–400.
- Aarts, W.M., R. Willemze, R.J. Bende, C.J.L.M. Meijer, S.T. Pals, and C.J.M. van Noesel. 1998. VH gene analysis of primary cutaneous B-cell lymphomas: evidence for ongoing somatic hypermutation and isotype switching. *Blood.* 92:3857–3864.
- Cook, G.P., and I.M. Tomlinson. 1995. The human immunoglobulin VH repertoire. *Immunol. Today.* 16:237–242.